



 Cite this: *RSC Adv.*, 2021, **11**, 30237

 Received 22nd May 2021  
 Accepted 31st August 2021

DOI: 10.1039/d1ra03978d

[rsc.li/rsc-advances](http://rsc.li/rsc-advances)

# Layered double hydroxide-based nanocomposite scaffolds in tissue engineering applications

 Burcin Izbudak,<sup>†a</sup> Berivan Cecen,<sup>†bcd</sup> Ingrid Anaya,<sup>†e</sup> Amir K. Miri,<sup>bc</sup> Ayca Bal-Ozturk <sup>\*af</sup> and Erdal Karaoz<sup>\*agh</sup>

Layered double hydroxides (LDHs), when incorporated into biomaterials, provide a tunable composition, controllable particle size, anion exchange capacity, pH-sensitive solubility, high-drug loading efficiency, efficient gene and drug delivery, controlled release and effective intracellular uptake, natural biodegradability in an acidic medium, and negligible toxicity. In this review, we study potential applications of LDH-based nanocomposite scaffolds for tissue engineering. We address how LDHs provide new solutions for nanostructure stability and enhance *in vivo* studies' success.

## 1. Introduction

With the development of nanotechnology, biomaterials with nanoscale features have been commonly designed to be used in drug delivery and artificial matrices.<sup>1</sup> The potential of various nanomaterials, such as carbon nanotubes,<sup>2,3</sup> graphene oxide nanosheets<sup>4,5</sup> and nanoclays, (*i.e.* halloysite nanotubes and kaolinite nanosheets)<sup>6–8</sup> has been extensively investigated. Among numerous nanomaterials, LDH nanoparticles, nano-sized inorganic clay, have attracted the enormous attention of researchers worldwide due to their advantages, such as biocompatibility, antigenicity, acceleration of the tissue regeneration, biodegradability, bioactive interface, and controlled release of drugs. LDHs is a commonly used nanomaterial in nanomedicine and bioengineering with a unique 2D structure, controllable particle size,<sup>9</sup> and anion exchange capacity,<sup>10</sup> pH-sensitive solubility, thermal stability,<sup>11</sup> chemical stability,<sup>12</sup> high-drug loading efficiency,<sup>13</sup> efficient drug delivery,<sup>14</sup> low toxicity,<sup>15</sup> and biocompatibility properties.<sup>16</sup> LDHs are 2D

hydroxide compounds having width sizes less than 100 nm, and their anionic exchange capacity and organic/inorganic intercalations make them great carriers for drugs and biological agents.<sup>17</sup> As a storage matrix, the release of different anionic species into the structure can be controlled by acidic pH.<sup>18</sup> They are commonly shown as  $[M^{2+}_{1-x} M^{3+}_x (OH)_2] [A^{n-}]_{x/n} \cdot zH_2O$ , where divalent cations ( $M^{2+}$ ) are  $Mg^{2+}$ ,  $Fe^{2+}$ , or  $Co^{2+}$ ; trivalent cations ( $M^{3+}$ ) are  $Al^{3+}$ ,  $Fe^{3+}$ , or  $Gd^{3+}$ ; and non-framework and exchangeable anions ( $A^{n-}$ ) are  $Cl^-$ ,  $CO_3^{2-}$ ,  $NO_3^-$ , *etc.*<sup>19</sup> LDHs have a layered crystal structure and consist of a positively charged host layer, since  $M^{3+}$  partially replaces  $M^{2+}$  anions, alternating with interlayers containing exchangeable anions hydrated with water molecules<sup>19,20</sup> (Fig. 1A). The LDHs' synthesis methods are co-precipitation, ion exchange in solution, sol-gel, hydrothermal, urea hydrolysis, and the reconstruction/rehydration method (*i.e.*, memory-impact method).<sup>19,21</sup> The co-precipitation method is the simplest one, in which basic solutions of LDHs can be easily prepared in high purity and crystallinity.<sup>21,22</sup> The rich-OH ionic groups and natural positive charges in the structure enable the formation of 3D nano-hybrid structures through interactions with molecules and nanomaterials. Surface modification can customize for core, shell, dot-coated, and targeting in the carrier system.<sup>23</sup>

Different characterization methods were used to study LDHs with biological components, as shown in Fig. 1B and C.<sup>15,24</sup> The three main groups of LDHs used in biomedical applications are (I) organic agents entrapped between the interlayer of LDHs, (II) the dispersion of LDHs into a polymeric network, and (III) LDHs intercalated with biological molecules.<sup>25</sup> There have been numerous studies on these three groups, such as bone tissue engineering;<sup>26</sup> however, there are limited tissue engineering studies. Here, we introduced the potential applications of LDHs in tissue engineering applications. We focus on biocompatibility, antibacterial properties, and osteogenic differentiation associated with LDHs in tissue engineering, and we discuss

<sup>a</sup>Department of Stem Cell and Tissue Engineering, Institute of Health Sciences, Istinie University, Istanbul, Turkey. E-mail: aycabal@gmail.com; ekaraoz@istinie.edu.tr

<sup>b</sup>Biofabrication Lab, Department of Mechanical Engineering, Rowan University, Glassboro, NJ, 08028, USA

<sup>c</sup>School of Medical Engineering, Science and Health, Rowan University, Camden, NJ, 08103, USA

<sup>d</sup>Department of Molecular Biology and Genetics, Faculty of Engineering and Natural Sciences, Istinie University, 34010, Zeytinburnu, Istanbul, Turkey

<sup>e</sup>Department of Bioengineering, Tecnológico de Monterrey, Campus Monterrey, CP, 64849, Monterrey, Nuevo León, México

<sup>f</sup>Department of Analytical Chemistry, Faculty of Pharmacy, Istinie University, Istanbul, Turkey

<sup>g</sup>Department of Histology and Embryology, Faculty of Medicine, Istinie University Istanbul, Turkey

<sup>h</sup>Center for Regenerative Medicine and Stem Cell Research and Manufacturing (LivMedCell), Istanbul, Turkey

<sup>†</sup> Equal contribution.



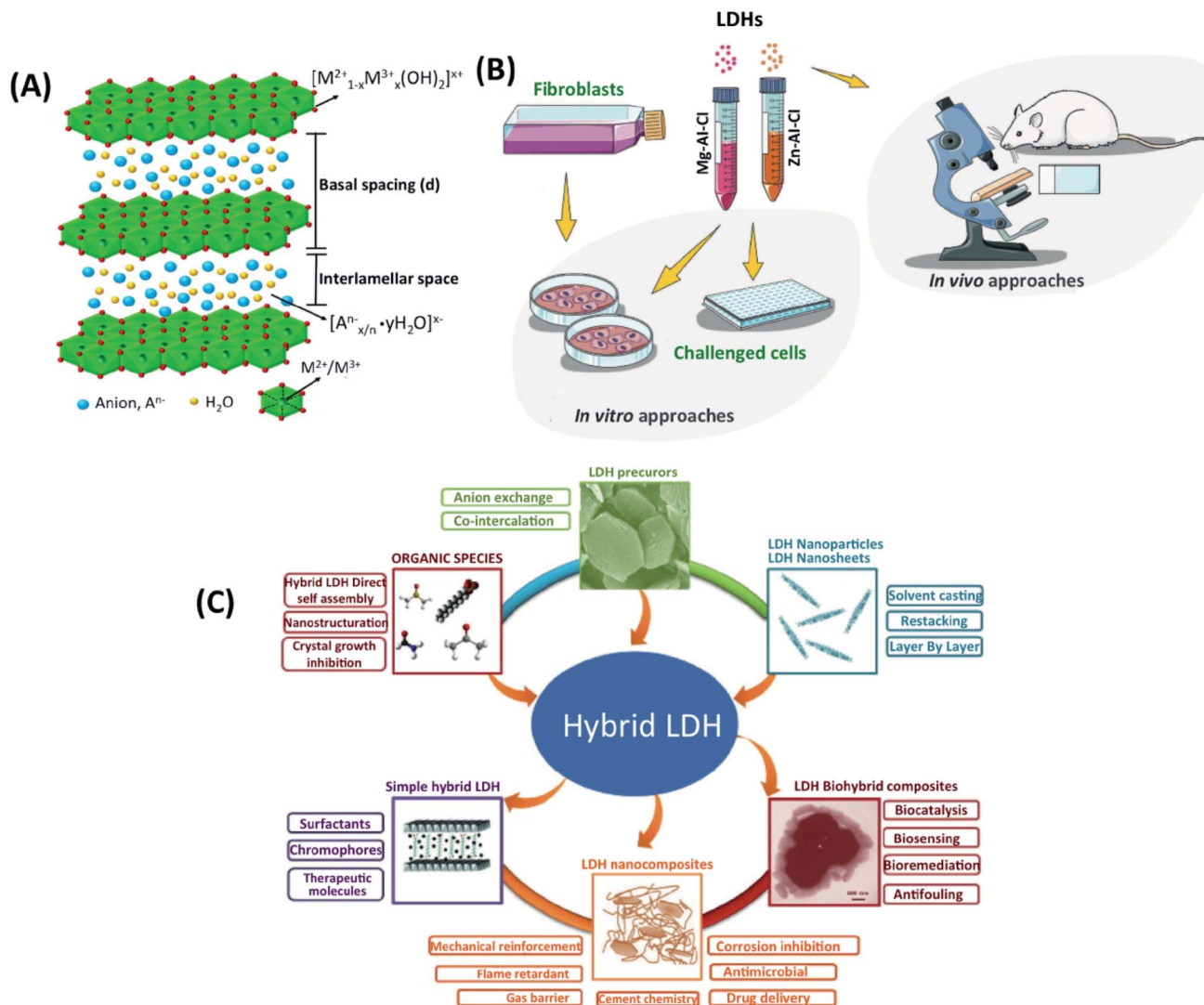


Fig. 1 (A) The general structure of LDHs. This figure is reproduced from ref. 19 with permission from Elsevier, copyright 2017. (B) The available design of LDHs experiments. This figure is reproduced from ref. 15 with permission from John Wiley and Sons, copyright 2019. (C) Current research on LDHs, and the existing category of LDH precursors, nanoparticles, hybrids, and biohybrid composites. This figure is reproduced from ref. 24 with permission from John Wiley and Sons, copyright 2017.

current challenges and future perspectives. The manuscript is divided into four sections. First, the bioactivity of LDHs in different systems is discussed. Second, the efficiency of LDHs for antibacterial properties is well explained for various cases. Third, their applications in bone engineering are shown in detail. Lastly, future trends and perspectives are discussed. In this paper, we introduce the recent advances of LDHs for bone and cartilage tissue-engineered scaffolds in regenerative medicine as drug delivery carriers.

## 2. Bioactivity of LDHs

Hydrogels can be designed to mimic the extracellular matrix of soft tissues for delivery nanocarriers and cellular scaffold applications in regenerative medicine. In most cases, they only offer physical support, and they need to be biofunctionalized for

cell spreading, proliferation, and differentiation. The toxicity levels for LDHs have been tested for various cellular components (Table 1). These hydrogels' bioactivation involves the copolymerization of acrylate functional peptides cross-linked with poly(ethylene glycol) (PEG) derivatives. Huang *et al.*<sup>27</sup> describe bioactive nanocomposite PEG hydrogel preparation cross-linked by polydopamine-coated layered double hydroxides (PD-LDHs). The PEG hydrogel with the catechol-rich PD-LDH showed tunable mechanical strength, bioactivity and bioadhesion, self-healing ability and supported the osteogenic differentiation of human mesenchymal stem cells.

Bioadhesion is another critical consideration in designing hydrogels for tissue regeneration. The hydrogels' tight adhesion potentially leads to better integration with the surrounding biological tissues, facilitating infiltration of bioactive molecules and cells promoting tissue healing.<sup>27</sup> The cellular and



## Review

Table 1 Toxicity data for LDHs with different cell cultures

| LDH type/molar ratio | Size (nm) | Conc. ( $\mu\text{g mL}^{-1}$ ) | Cell types                                       | Assay (test)  | Results                                                                       | Ref. |
|----------------------|-----------|---------------------------------|--------------------------------------------------|---------------|-------------------------------------------------------------------------------|------|
| Mg–Al LDHs 2 : 1     | 50–100    | 40                              | Human embryonic kidney cells (293T)              | MTT           | The non-toxic effect, more than 80% viability after three days                | 31   |
| Zn–Al LDHs 2 : 1     | —         | 5–150                           | Mouse fibroblast cells (3T3)                     | MTT           | 90% viability at 100 $\mu\text{g mL}^{-1}$ concentration                      | 32   |
| Mg–Al LDHs 3 : 1     | 80–90     | 20                              | Human cervical cancer                            | MTT           | Very low toxicity after 72 h treatment                                        | 33   |
| Mg–Al LDHs 4 : 1     | —         | 50                              | Breast (MCF-7), HeLa, and fibroblast (3T3) cells | MTT           | Non-toxic effect                                                              | 34   |
| Mg–Al LDHs 3 : 1     | —         | 40                              | GES-1, MKN45 and SGC-7901 cells                  | MTT           | Non-toxic effect                                                              | 35   |
| Zn–LDHs              | —         | 25–0.195                        | Monkey kidney (Vero-3) cells                     | MTT           | 92% viability at 25 $\mu\text{g mL}^{-1}$ concentration                       | 36   |
| Zn–LDHs              | —         | 5–500 $\text{mg kg}^{-1}$       | Rat                                              | Oral toxicity | Non-clinical toxicity and animal demise at 5–500 $\text{mg kg}^{-1}$ dose     | 37   |
| Zn–Al LDHs 2 : 1     | —         | 25–800                          | PC12 cells                                       | MTT           | Low toxic effect at 800 $\mu\text{g mL}^{-1}$ concentration                   | 38   |
| Mg–Al LDHs 3 : 1     | 100       | 2–40                            | Mouse embryonic stem cells (mESC)                | MTT           | Excellent biocompatibility                                                    | 39   |
| Mg–Al LDHs 3 : 1     | 50, 100   | 10–400                          | Mouse embryonic stem cells (mESC)                | MTT           | No significant cytotoxicity at a concentration up to 40 $\mu\text{g mL}^{-1}$ | 40   |
| Mg–Al LDHs 2 : 1     | —         | 1–1000                          | Human leukemia cells (HL-60)                     | MTT           | Non-toxic effect                                                              | 41   |

biochemical properties of LDHs were evaluated, in which two combinations of LDHs (Mg–Al–Cl and Zn–Al–Cl) with different concentrations were tested (Fig. 2A). Standard viability analysis (MTT) was performed to assess the acceptable range of concentrations. A range of 0.002–0.2  $\text{mg mL}^{-1}$  did not lead to a half-maximal inhibitory concentration (IC<sub>50</sub>) value within 24 h. Mg–Al–Cl showed a better cell growth pathway for fibroblast adhesion when compared to Zn–Al–Cl (Fig. 2B and C). The effects of the culture media on the shape of LDHs were stated to be negligible. The results indicate that LDHs guide cellular adhesion, migration, proliferation and delineate new advances on the biomaterial area implemented for soft tissue bioengineering.<sup>26</sup> Baek *et al.* examined the cytotoxic effects of two different types of LDHs, Mg–Al–CO<sub>3</sub>, and Mg–Al–Cl, on human lung alveolar carcinoma epithelial cells (A549) and normal human lung alveolar epithelial cells (L-132). They prepared LDHs by the molar ratio of Mg/Al = 2 using the co-precipitation process. The production of reactive oxygen species (ROS) was then determined with a cell permeable fluorescent probe, 2',7'-dichlorofluorescein diacetate (H2DCFDA). The human lung alveolar carcinoma epithelial cells (A549) and normal human lung alveolar epithelial cells (L-132) were treated with LDHs at concentrations up to 1000  $\mu\text{g mL}^{-1}$  for 72 hours. The stability and toxicity of LDHs were investigated for the effect of the proliferation of L-132 and A549 cell lines. Mg–Al–CO<sub>3</sub> LDHs with a size of 200 nm led to significant ROS in the A549 cell line. Mg–Al–CO<sub>3</sub> LDHs showed higher toxicity in comparison to Mg–Al–Cl LDHs.<sup>28</sup>

Choi *et al.*<sup>29</sup> evaluated the toxicity of anionic clay, layered metal hydroxide nanoparticles, two human lung epithelial cells, and carcinoma A549 normal L-132 cells. They determined it to be low tested at the concentrations used (<250  $\mu\text{g mL}^{-1}$ ) within 48 h in comparison with other inorganic nanoparticles, such as silica, iron oxide, and carbon nanotubes. Higher concentrations (250–500  $\mu\text{g mL}^{-1}$ ) of LDHs for 72 h resulted in an inflammatory response with oxidative stress and membrane damage. Therefore, oxidative stress can be caused depending on the type of nanoparticle,<sup>30</sup> concentration, and exposure time, affecting the toxicity.

Peng *et al.* developed the different LDHs (Mg–Al, Mg–Fe, Zn–Al, and Zn–Fe) to apply bone implants. They evaluated the feasibility of the LDH with biological functional elements as bone implants,  $\text{M}^{2+}$  was chosen for being essential for bone regeneration,  $\text{Zn}^{2+}$  was selected for skeletal development and antibacterial activity, while  $\text{Al}^{3+}$  and  $\text{Fe}^{3+}$  for their low toxicity. Osteoblast-like cells (MC3T3-E1), related to bone growth, and human umbilical endothelial cells (HUVECs) were investigated to determine the cytotoxic activity LDHs. LDHs with specific amounts in the form of extracts or suspensions were treated. Mg–Al and Mg–Fe LDHs indicated higher cell viability than Zn–Al and Zn–Fe LDHs. The concentrations of Zn–Al LDHs extract higher than 1.11  $\text{mg mL}^{-1}$  led to significant toxicity. The apparent toxicity of Zn–Fe LDHs was observed at an extract concentration of 123.5  $\mu\text{g mL}^{-1}$ . Unlike the extract, Zn–Al and Zn–Fe LDHs suspensions showed more severe toxicity to HUVEC and MC3T3-E1 than Mg–Al Mg–Fe LDHs when the



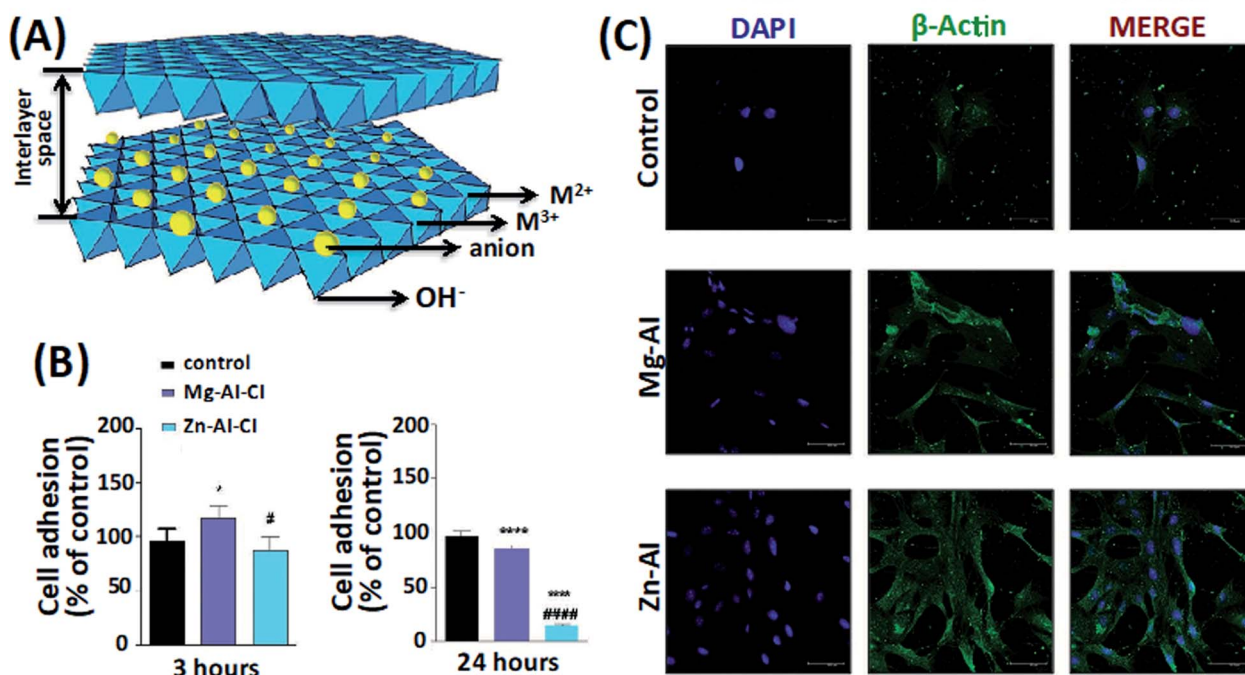


Fig. 2 (A) The LDHs structure. (B) The effect of two compositions and types of LDHs, Mg-Al-Cl and Zn-Al-Cl LDHs, on fibroblast adhesion. (C) The cell morphologies on the LDHs constructs after 24 hours. This figure is reproduced from ref. 26 with permission from John Wiley and Sons, copyright 2019.

concentration of their breaks was higher than  $41.2 \mu\text{g mL}^{-1}$ .<sup>42</sup> The present study evaluated the mechanical properties, as well as cytotoxicity and antibacterial ability. Zn-Fe LDHs is the most suitable for a bone implant. It has the highest hardness and elastic modulus; a mismatch in the elastic modulus between the bone and the implant would lead to stress shielding, which causes bone resorption after surgery.

One major issue of bone implants is the formation of bacteria films. Thus, it is essential to engineer the LDHs with antibacterial potential to allow their osseointegration. It has been reported in the literature that Zn damages the membrane and nucleic acid and denatures the bacteria proteins and enzymes. Therefore, bacteria (*E. coli* and *S. aureus*) showed lower tolerance concentration of Zn-Al LDH and Zn-Fe LDH. Soo *et al.* reported that Mg-Al and Zn-Al LDHs at concentrations up to  $500 \mu\text{g mL}^{-1}$  had no toxic effects within 48 hours in various cell lines and red blood cells.

The findings revealed that Zn-Al LDHs induced much more serious membrane damage and hemolysis than Mg-Al LDHs. Based on these findings, Mg-Al LDHs in various sizes (50, 100, 200, 350 nm) were tested. Mg-Al LDHs at concentrations up to  $500 \mu\text{g mL}^{-1}$  were treated with A549 cells for 48 hours. While Mg-Al LDHs of 50 nm in size treated with A549 cell lines were found to be more toxic than larger nanoparticles, Mg-Al LDHs in size range from 100 to 200 nm were found to show very low cytotoxicity. Even LDHs of 50 nm in size, which is a toxic effect *in vitro*, did not result in body weight loss or mortality *in vivo*. On the other side, in *in vivo* studies, all LDHs groups did not cause any mortality or weight loss of  $600 \text{ mg kg}^{-1}$ . The

assumption that LDHs are attractive biocompatible biomaterials for biological and medical applications has been confirmed.<sup>43</sup>

Cunha *et al.* (2016) assessed the biocompatibility, bio-integration, non-immunogenic feature, and antigenicity properties of Mg-Al and Zn-Al LDHs tablets post-implanting intramuscularly in rat abdominal as it allows to test the activation of the whole immune response in few 7 days and the rejection process by fibrous capsule formation in a more extended period, 28 days through the microcirculation.<sup>44</sup> A stroboscopic LED video-microscopy was used to observe the micro-circulation patterns of the host tissues around LDHs. The two types of LDHs had 80–100 nm, and the co-precipitation process produced them. The sterilized LDHs were implanted in rats' abdominal walls, and the results showed that LDHs had appropriate biocompatibility on day 7. Histological tests evaluated the reaction of the LDHs with host tissue post-implantation neo-vascularized connective tissue was observed around the treated area (Fig. 3). The real-time observation showed that muscle tissues implanted with Mg-Al and Zn-Al LDHs support non-immunogenic properties, adequate extracellular matrix remodeling to the desired collagen type wound healing according to the tablet biophysical composition. This healing process involves the deposition of collagen and fibronectin fibers; the Zn-Al LDH tablet sample exhibited a predominance of collagen type-III fibers. Besides, the alkaline pH buffering behavior of the LDHs promoted normal cellular response as chemotaxis, respiratory activity, and proliferative capacity of leukocytes; thus, good tissue repair response. These





Fig. 3 Histological images of the implants after 28 days show the final tissue reconstruction and the persistence of the implanted LDH constructs. This figure is reproduced from ref. 44 with permission from Springer Nature, copyright 2016.

results suggest that they can be used in biomedical applications for drug delivery.<sup>44</sup>

Nanocomposite-based hydrogels are enhancing the mechanical and chemical properties of hydrogels and expanding their biomedical applications. When encapsulated with inorganic nanoparticles, they have shown excellent biocompatibility, stability, and mechanical properties compared to new hydrogels due to the remarkable physical, chemical, and biological features of inorganic nanoparticles. Wang *et al.* mixed LDHs and nanohydroxyapatite (HAp) to develop a porous nanocomposite hydrogel made of poly(*N*-isopropyl acrylamide) (PNIPAm/LDHs/HAp), which showed superior hemocompatibility, enhanced mechanical strength, and reversible swelling/deswelling properties. These results support that the developed hydrogel embedded with LDHs and HAp has excellent potential for tissue engineering and clinical practices.<sup>45</sup>

### 3. Antibacterial properties of LDHs

Antibacterial properties in scaffolds yield significant success and adaptation in clinical applications.<sup>46</sup> The antimicrobial activity of scaffolds allows controlling surgical infections and reducing any antimicrobial agents' injection.<sup>47</sup> An ideal implant should have an antibacterial ability while providing cell

adhesion and proliferation. Metallic ions such as Ag, Zn, Ti, Sr can be incorporated into scaffolds to accelerate tissue regeneration with minimal infections.<sup>48</sup> These metallic ions cause ROS production in antibiotic-resistant bacteria, causing membrane and DNA damage and inactivating metabolic proteins such as respiratory enzymes.<sup>49</sup> LDHs can decrease the number of nutrients in the culture media by adsorbing on the surface of particles. Differences in the environment's physicochemical features occur, inhibit bacteria's growth (Fig. 4A). In the meantime, electrostatic interactions between the cationic LDHs and negatively charged bacterial surface can cause bacterial growth inhibition.<sup>50</sup>

LDHs also show strong ion-exchange potential and porous structures; for example, Zn ion-based LDHs exhibit strong antibacterial properties leading to bone implant's fast regeneration.<sup>51</sup> Peng *et al.* have recently reported an alternative method by preparing Mg–Al, Mg–Fe, Zn–Al, and Zn–Fe LDHs. Extract and suspension forms of Zn–Al LDHs and Zn–Fe LDHs displayed a better antibacterial impact on Gram-positive *S. aureus* and Gram-negative *E. coli* compared to the Mg–Al and Mg–Fe LDHs. Zn–Al and Zn–Fe LDHs into the scaffold showed higher success and potential for the application of antibacterial implants.<sup>42</sup> The bacterial resistance to antibiotics increases over time. Gohi *et al.* developed a new organic–inorganic hybrid



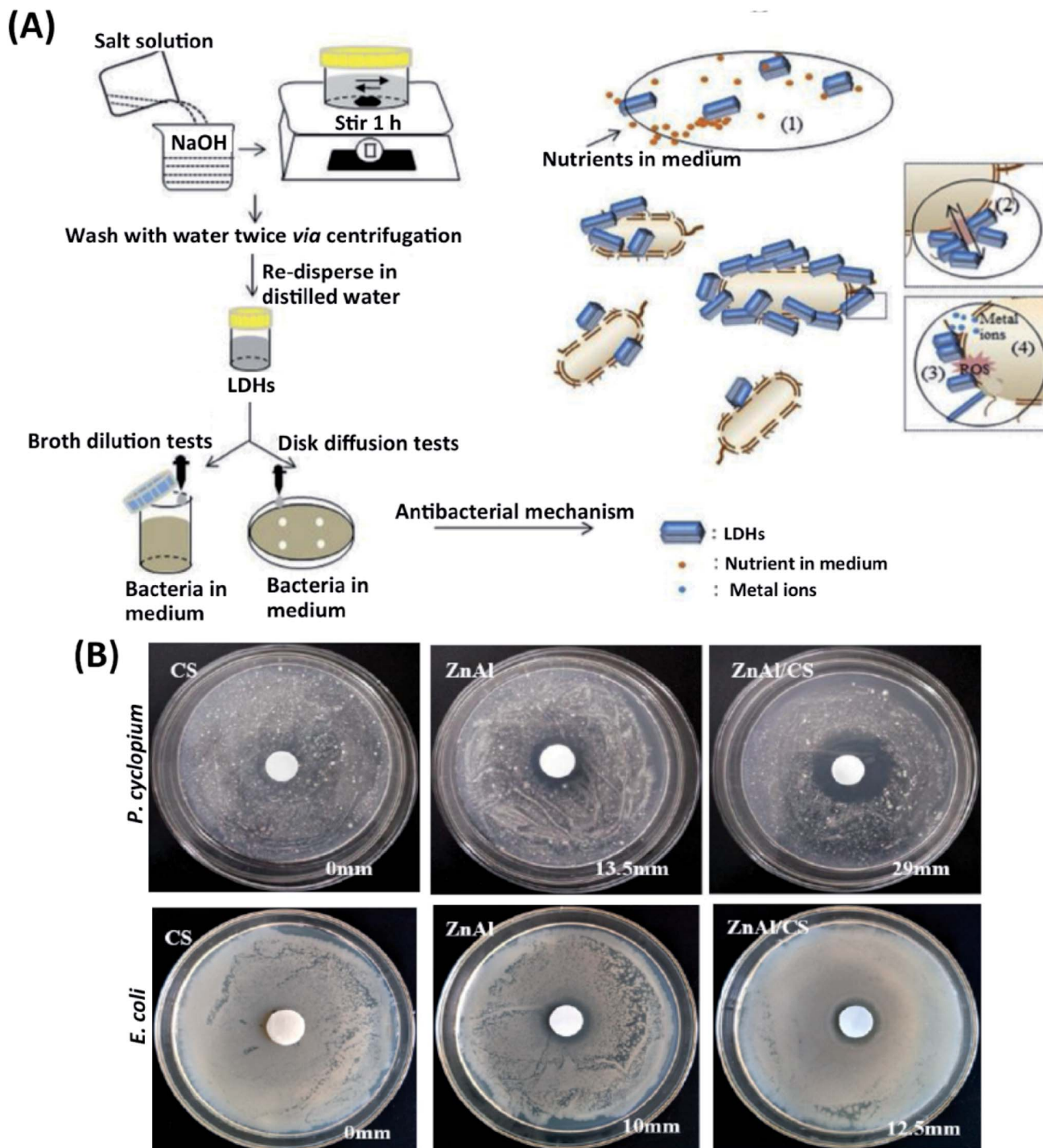


Fig. 4 (A) A schematic illustration of an antibacterial-experimental strategy and possible antibacterial mechanism of LDHs. This figure is reproduced from ref. 50 with permission from Elsevier, copyright 2020. (B) Effects of CS, Zn–Al LDHs, and CS/Zn–Al LDHs against *P. cyclopium* and *E. coli*. This figure is reproduced from ref. 52 with permission from MDPI, copyright 2019.

biomaterial consisting of Zn–Al LDHs/chitosan (CS). With the release of  $Zn^{2+}$  and  $Al^{3+}$  metal ions from Zn–Al LDHs/CS hybrid biomaterial, an increase of the inhibition zone of 41.6% against *E. coli* and almost 100% for *Penicillium cyclopium* (*P. cyclopium*) was observed (Fig. 4B).<sup>52</sup> In another study, an antibacterial environmentally friendly polyurethane (WPU)-based composite

was synthesized with Zn–Al LDHs, and ZnO, ZnO LDHs have been reported to inhibit bacteria growth and their proliferation effectively. The antibacterial effect was assessed for composite biomaterials against Gram-negative *E. coli* and Gram-positive *S. aureus*. The results show that WPU embedded with ZnAl-LDHs/ZnO has solid antibacterial potential. The antibacterial activity



of WPU/Zn–Al LDHs/ZnO composite exists on two mechanisms. First, ZnO activates intercellular ROS such as hydrogen peroxide ( $\text{H}_2\text{O}_2$ ) and strengthens oxidizing agents, damaging the bacterial cells. Second,  $\text{Zn}^{+2}$  ions in LDHs penetrate the bacterial membrane while altering the cell membrane's permeability and causing individual proteins' denaturation.<sup>53</sup> In another similar study, the proliferation of *S. cerevisiae*, *S. aureus*, and *E. coli* has been severely inhibited by Zn–Ti LDHs and evaluated the size-dependent antibacterial behavior of Zn–Ti LDHs.  $\text{Ti}^{+3}$  cations in Zn–Ti LDHs with a size of 40 nm showed a more active antibacterial effect than metal oxide and  $\text{TiO}_2$ . Zn–Ti LDHs killed more than 95% of the bacteria and exhibited excellent antibacterial action.<sup>54</sup>

Since silver has antibacterial properties, composite biomaterials have been preferred in many studies. Mehdi *et al.* focused on the antibacterial effect of silver and LDHs in the carboxy-methyl-cellulose (CMC)-based hydrogel. CMC nanocomposites' antibacterial effect includes Mg–Al, Ni–Al, Zn–Al, and Al LDHs against *E. coli* and *S. aureus* bacteria has been investigated. Cu–Al LDHs/CMC and Zn–Al LDHs/CMC nanocomposites showed more antibacterial effects than nanocomposites, including Mg–Al Ni–Al LDHs. This is because of Cu and Zn ions' antibacterial properties released from Cu–Al LDHs/CMC and Zn–Al LDHs/CMC constructs. The inhibition zone for Cu–Al LDHs/CMC and Zn–Al LDHs/CMC against *E. coli* decreased after 3 days. On the other hand, they displayed better potential towards *S. aureus* and kept their antibacterial impact for more than 2 weeks.<sup>55</sup> Gabriela *et al.* reported the antibacterial effects on Zn–Al LDH, Ag/Zn–Al LDHs, and AgNP against *S. aureus* and *E. coli*. The superior stability and efficacy of the antibacterial potential of Ag/Zn–Al LDHs are possibly owing to the power of the LDHs structure to adsorb microorganisms; thus, enabling strong interactions with the silver from the surface.<sup>56</sup>

Ahmed *et al.* successfully used Zn for antibacterial properties of polyaniline (PAn) nanocomposite, including Zn–Al LDHs. The antimicrobial activity of PAn/Zn–Al LDHs nanocomposites was assessed against Gram-positive (*Staphylococcus aureus*), Gram-negative (*Pseudomonas aeruginosa*) bacteria, and fungi (*Candida albicans*). The results reported that PAn/Zn–Al LDHs prevented bacteria and fungi from stuck on the surface and provided antimicrobial effects by growing the ability.<sup>57</sup> In another study, Penicillin G (PNG)-loaded Zn–Al LDHs prepared to make prolonged antibacterial potential against *E. coli*. In the meantime, the released  $\text{Zn}^{+2}$  ions from Zn–Al LDHs had an antibacterial ability by significantly improving the antibacterial effect of PNG.<sup>58</sup>

Jin *et al.* intercalated an anticancer drug 5-fluorouracil/cyclodextrin (5-FU/CMCD) into a Zn–Al LDH. The drug release time was prolonged and controlled by the hydrophobic environment of the CMCD cavity and by the durability of the LDH. Therefore, the release behavior of 5-FU from 5-FU/CMCD-LDH composite could be modulated by a change in the environmental pH value.<sup>1</sup> Other pharmaceutical compounds such as ibuprofen, fenbufen, and diclofenac have been incorporated into LDHs and exhibited LDH-based tunable drug delivery systems' feasibility.<sup>1,9,19</sup>

## 4. Osteogenic differentiation properties of LDHs

The bone tissue that forms the skeletal system is protected and renewed by the proliferation of osteoblasts and osteoclasts. The primary cells that provide bone formation are osteoblasts, which allow the shaping of new bone tissue and mineralization with ECM. Throughout different experiments, embryonic stem cells (ESCs), pluripotent stem cells (PSCs), MSCs, and bone marrow (BM-MSCs) are commonly used to differentiate into osteoblasts.<sup>47</sup> Genes that provide osteogenic differentiation have many transcription factors and proteins. The primary transcription factor is runt-related transcription factor 2 (RUNX2), which provides the expression of osteocalcin (OCN), collagen type 1 (COL1A1), and osteocalcin (OCN) proteins.<sup>59</sup> Another specific transcription factor is alkaline phosphatase (ALP), which measures osteoblasts' ability to mature and regenerate bone.<sup>60</sup> Tissue engineering creates scaffolds that can regenerate bone by stimulating genes, mimicking the bone structure, and providing osteogenesis.<sup>61</sup> Due to its ionic content and layered structure, LDHs have been recently preferred in bone scaffolds reducing mechanical strength, producing  $\text{Mg}^{+2}$ , and forming an alkaline micro-environment (Table 2).<sup>62</sup> During  $\text{Mg}^{+2}$  ions released from LDHs, osteogenic cells' integrin expression is upregulated,<sup>63</sup> and  $\text{Mg}^{+2}$  ions have a synergistic effect on stem cells' ALP activity and osteogenesis pathways.<sup>64</sup> During osteoclastogenesis, LDHs promote osteoblastic phenotype by up-regulating osteogenic marker genes, RANKL and OPG. The pathways of signaling in response to LDHs are actualized by osteoblasts.<sup>61</sup> In conclusion, LDHs can be considered a significant stimulus during osteoclastogenesis and preferred to repair bone defects.

The microstructure and chemical composition of gelatin/LDHs/Hap-based scaffolds were similar to native bone structures. The gelatin/LDHs/HAP-based scaffold's bone regeneration ability was shown in orthopedic and regenerative surgery for bone healing.<sup>65</sup> For significant bone defects to restore healthy bone, engineered scaffolds should be biocompatible and support osteogenic differentiation without causing infection. Dandan *et al.* successfully prepared a new nanocomposite scaffold by combining Ag-laden MgSrFe LDHs with CS (CS/Ag-MgSrFe LDH). CS/Ag-MgSrFe nanocomposite scaffold was non-toxic on human bone marrow-derived mesenchymal stem cells (hBMSCs). The cells showed enhanced spread, proliferation, and adhesion on the scaffold. Due to the release of  $\text{Sr}^{2+}$  ions from LDHs, ALP RUNX2 and BMP-2 expression increased. CS/Mg–Fe LDHs were compared with CS/Ag-MgSrFe LDH nanocomposite scaffold, and data indicated that the nanocomposite scaffolds containing Ag and Sr elements support osteogenic differentiation. Besides, Ag components in LDHs provided excellent bone formation, which gained antibacterial activity and kept osteoinductivity (Fig. 5C).<sup>66</sup>

Heqin *et al.* utilized a new nanocomposite consisting of PEG-based hydrogel by using polydopamine-coated LDHs (PD-LDHs). The catechol-rich PD-LDHs nanosheets not only possessed strong bioadhesive properties in the aqueous



Table 2 LDHs major applications for bone regeneration and tissue engineering

| LDH type                                         | Application                          | Cell line/tissue model                          | Results                                                                                                                                           | Ref. |
|--------------------------------------------------|--------------------------------------|-------------------------------------------------|---------------------------------------------------------------------------------------------------------------------------------------------------|------|
| Mg–Al, Mg–Fe, Zn–Al, and Zn–Fe LDHs              | Bone implantation                    | MC3T3-E1                                        | Zn–Fe had the highest hardness and elastic modulus, most suitable avoiding bone resorption after surgery.                                         | 42   |
| Mg–Fe LDH                                        | Bone implantation                    | rBMSCs                                          | Mg–Fe LDH films on titanium increased the ALP activity, collagen secretion, ECM mineralization, and proliferation and osteogenic differentiation. | 70   |
| Cs/Ag-laden MgSrFe LDHs                          | Bone regeneration                    | hBMSCs                                          | ALP, RUNX2 and BMP-2 expression increased. Ag and Sr elements supported osteogenic differentiation and bone formation.                            | 66   |
| PD-LDHs                                          | Bone regeneration                    | hMSCs                                           | Increased the mechanical strength, bioadhesion, spreading and osteogenic differentiation of hMSCs.                                                | 67   |
| Mg–Al LDHs                                       | Bone regeneration                    | rBMSCs and MC3T3-E1                             | Mg–Al LDHs and titanium's alkaline environment regulated the oxidative stress, proliferation, and ALP activities of osteoblast cells.             | 63   |
| CS/Mg–Al LDHs/PFT- $\alpha$                      | Bone regeneration                    | hBMSCs                                          | PFT- $\alpha$ induced the GSK3- $\beta$ /y-catenin pathway and showed an enhancing effect on hBMSC differentiation.                               | 71   |
| Mg–Al and Zn–Al LDHs                             | Bone regeneration                    | Preosteoblasts                                  | Enhanced osteocalcin (OCN), RUNX2, and Osterix (OSX). Reprogramming the mineralization and osteoclast-osteoblast fusion.                          | 61   |
| Vitamin D3 (VD3) LDH-Hap                         | Bone regeneration                    | Hap containing scaffolds (LHG and LHGD)         | Increased mechanical strength and ossification.                                                                                                   | 73   |
| (PAEU/LDH/hGH) Adenosine (Ado)-loaded Mg–Al LDHs | Bone regeneration                    | HCT-166 cell lines and <i>in vivo</i> rat model | Osteogenic differentiation of stem cells through the activation of the adenosine a2b receptor. Repaired rat tibia after six weeks.                | 68   |
| Bis-GMA and TEGDMA with Mg–Al-F LDH              | Dental applications                  | hDPSCs                                          | Fluoride release increased the hDPSCs and ALP activity, an odontoblastic differentiation.                                                         | 61   |
| Mg–Al LDHs                                       | Tissue regeneration and drug release | Calvarial osteoblasts isolated from mice        | High ALP potential and bone nodule, Mg–Al LDHs supported anti-inflammatory and osteogenic activity.                                               | 62   |
| PAG-PA-PD with Mg–Al LDHs                        | Chondrogenic differentiation         | TMSCs                                           | Increased mRNA and protein levels of type II collagen and SOX9 in TMSCs                                                                           | 65   |

environments but also increased the mechanical strength of the obtained PEG-based hydrogel (Fig. 5A and B). It was seen that PD-LDHs cross-linked PEG-based nanocomposite hydrogel enhanced adhesion, spreading, and osteogenic differentiation of human derived mesenchymal stem cells (hMSCs). As a result, they carried out a nanocomposite hydrogel that can have incredible potency in regenerative medicine and open up a new way to design PEG-based nanocomposite constructs.<sup>67</sup>

Loredana *et al.* have explored the fundamental effects of fluoride ion-doped Mg–Al LDHs into hydrogel scaffolds. Bisphenol-A glycidyl dimethacrylate (Bis-GMA) and tri-ethylene glycol dimethacrylate (TEGDMA) combined with Mg–Al-F LDH. The addition of Mg–Al-F LDHs promoted the mechanical features of the hydrogel resin. Slow fluoride release from hydrogel increased human dental pulp stem cells (hDPSCs) and ALP activity, an early odontoblastic differentiation for 28 days. Considering these results, Mg–Al-F LDHs can be used as

a dental filler for tooth resins.<sup>68</sup> In another study, Michelle *et al.* developed a guided tissue regeneration membrane suitable for periodontology. The controlled release of drugs was achieved from tetracycline and alendronate from Mg–Al LDHs into the poly(lactic-co-glycolic acid) (PLGA)-based membranes. Calvarial osteoblasts isolated from mice were incubated with membranes for five weeks. A high ALP potential and bone nodule formation were detected, and Mg–Al LDHs supported anti-inflammatory and osteogenic activity as a bone graft.<sup>69</sup>

Tan *et al.* have designed a biomaterial to capture implant failures to investigate antibacterial and osteogenic activities on the different alkaline microenvironment of titanium surface-associated with Mg–Al LDHs. Cellular adhesion, proliferation, and ALP activities were examined on rat bone marrow mesenchymal stem cells (rBMSCs) and mouse osteoblast cells (MC3T3-E1) 1, 4 and 7 days. They also confirmed that Mg–Al LDHs and titanium's alkaline environment regulates the





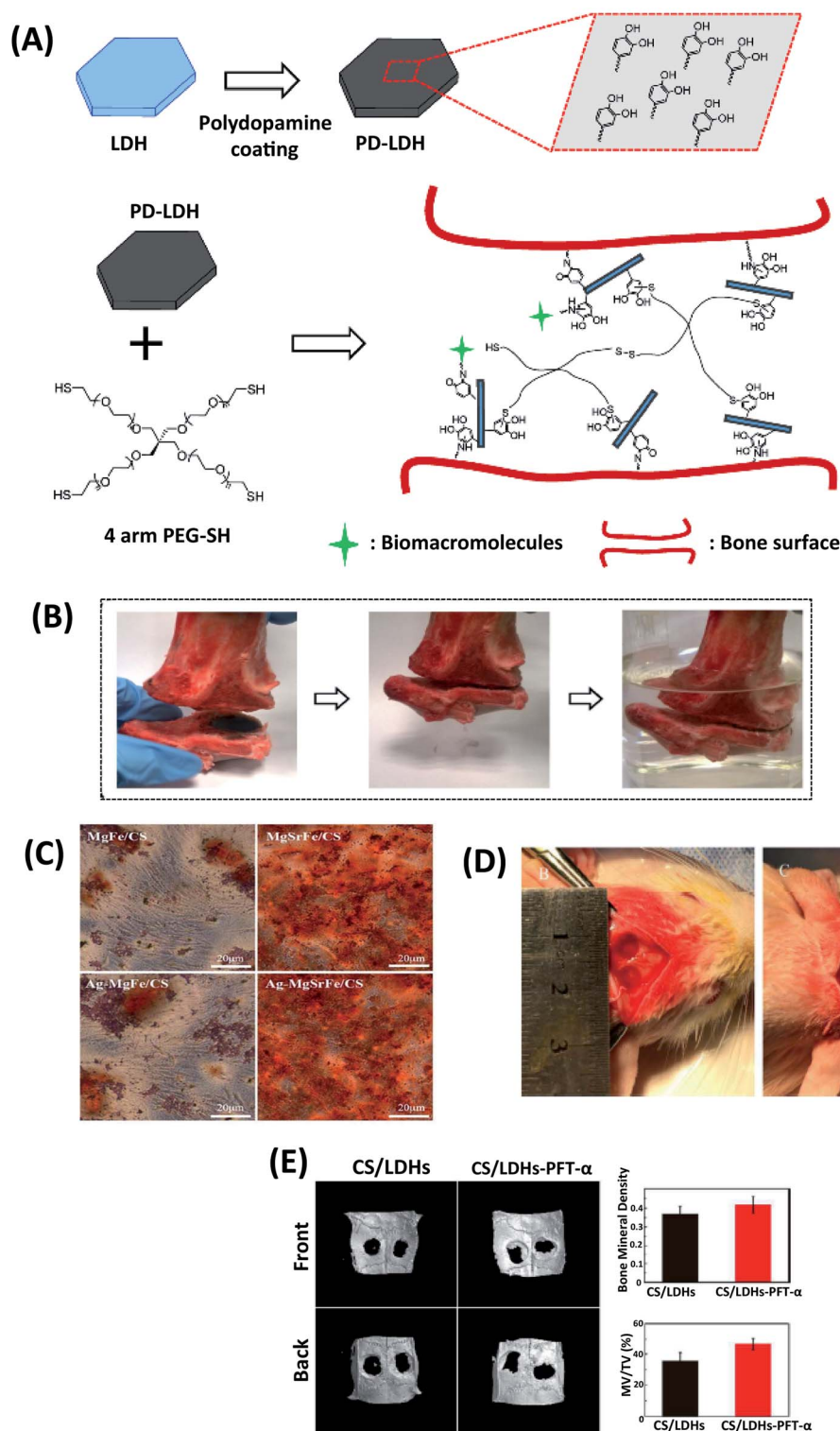


**Fig. 5** (A) Schematic illustration of polydopamine coating on LDHs and nanocomposite scaffold prepared by using 4-arm thiol-terminated polyethylene glycol (4-arm PEG-SH) and polydopamine-coated LDHs (PD-LDHs), which can carry biomacromolecules and act as the sealant for bone fracture. (B) The prepared nanocomposite scaffold has a strong sealant function for fractured bone pieces. This figure is reproduced from ref. 67 with permission from John Wiley and Sons, copyright 2016. (C) Alizarin Red staining for ECM mineralization of hBMSCs with CS/Mg-Fe, CS/Ag-MgFe, CS/MgSrFe, and CS/Ag-MgSrFe scaffolds. This figure is reproduced from ref. 66 with permission from John Wiley and Sons, copyright 2017. (D) The cranial defect was created, and CS/LDHs-PFT $\alpha$  or CS/LDHs constructs were placed in the cranial defects. (E) After twelve weeks, the defect region was examined using reconstructing micro-CT images. This figure is reproduced from ref. 71 with permission from RSC Pub, copyright 2017.





**Fig. 6** (A) *In vivo* implantation of gelatin/LDHs/HAp-based scaffold for bone tissue engineering application. This figure is reproduced from ref. 17 with permission from Elsevier, copyright 2017. (B) Schematic hGH loading in LDHs, and nanocomposite hydrogels. This figure is reproduced from ref. 74 with permission from RSC Pub, copyright 2015. (C) Schematic representation of Ado-loaded Mg–Fe LDHs preparation and their applications. The developed nanoparticulate platform synergistically induces the osteogenic differentiation of stem cells for healing of extended bone defects by co-delivering the Ado ligand and ligation stimulator (Mg ion). This figure is reproduced from ref. 64 with permission from Elsevier, copyright 2017.



oxidative stress, proliferation, and ALP activities of osteoblast cells.<sup>63</sup> In another study, Qianwen *et al.* produced Mg-Fe LDH films on titanium surfaces for challenging tissue implantation. Biocompatibility, proliferation, and osteoblast differentiation of the films were investigated on rBMSCs. They noticed that Mg-Fe LDH films on titanium increased the proliferation and osteogenic differentiation, ALP activity, collagen secretion, and ECM mineralization of rBMSCs, representing the encouraged applications as hard tissue implant materials.<sup>70</sup>

p53 has a key role in bone formation and metabolism. Scientists have recently reported that decreased p53 function is associated with bone formation. Pifithrin- $\alpha$  (PFT- $\alpha$ ) is a chemical inhibitor of p53 that prohibits p53 role for bone formation.<sup>72</sup> Yi-Xuan *et al.* investigated the different doses of PFT- $\alpha$  on the CS/Mg-Al LDHs composite scaffolds (CS/Mg-Al LDHs/PFT- $\alpha$ ) hBMSCs. They claimed that CS/Mg-Al LDHs/PFT- $\alpha$  scaffolds could be a novel strategy with natural bone regeneration functionality. For all that, they emphasized the increased COL1,  $\beta$ -catenin, and p53 by inducing the GSK3 $\beta$ /y-catenin pathway due to the release of PFT- $\alpha$ . Consequently, PFT- $\alpha$  induced the Wnt/ $\beta$ -catenin pathway and showed an enhancing effect on hBMSC differentiation (Fig. 5D and E).<sup>71</sup> In another study, the molecular mechanisms of Mg-Al and Zn-Al LDHs from preosteoblast to mature osteoblast led to enhanced osteocalcin (OCN), RUNX2, and Osterix (OSX). Mg-Al LDHs have a keynote regulation on OSX mRNA levels reprogramming the mineralization and osteoclast-osteoblast fusion balance with signal molecules.<sup>61</sup> Fateme *et al.* investigated the encapsulation of vitamin D3 on the gelatin-based scaffolds. LDH-HAP was combined with vitamin D3 to reinforce scaffolds. They observed that vitamin D3 plays a primary function in calcium accumulation, ALP activity regulation and osteoblastic expression. Reinforcement with vitamin D3 (VD3) the LDH-HAP into the scaffolds increased the mechanical strength and ossification, mimicking the mineral/organic structure of the natural bone and VD3 signaling effect. The HAP containing scaffolds (LHG and LHGD) avoided the adverse impacts of burst release, showed less water uptake, and recrystallized HAP, resulting in more bioactivity in these scaffolds. The more packed structures of LGD and LHGD lead to a decrease in the degradation rate due to less diffusion.<sup>73</sup>

Narendra *et al.* have prepared nano-bio hybrid injectable scaffolds (PAEU/LDH/hGH) to reduce the adverse effects of human growth hormone (hGH) inhibited by their early degradation short half-life. hGH was intercalated in the positively charged Mg-Al LDHs through an anion exchange technique (Fig. 6B). The injectable nano-biohybrid scaffold showed the delayed-hGH release diffusion by dual-ionic interactions as the scaffolds' pH and temperature sensitivity. Cytotoxicity using HCT-166 cell lines and *in vivo* rat model was used to study the scaffolds' biological response.<sup>74</sup>

Injectable hydrogels loaded with LDHs-hGH may be used effectively for sustained-hGH delivery to enhance biological efficaciousness and patient compliance.<sup>74</sup> Adenosine (Ado)-loaded Mg-Fe LDHs were also embedded within the injectable hydrogel to support the bone defect healing (Fig. 6C). The dual delivery of Ado and Mg ions from Ado-loaded Mg-Fe LDHs containing injectable hydrogel supported osteogenic

differentiation of stem cells through the synergistic activation of the adenosine A2b receptor was indicated. Furthermore, the injectable hydrogel promoted repairing rat tibia bone defects after six weeks. The serum hGH concentration remained high ( $\sim 1$  ng mL<sup>-1</sup>) with the LDH-hGH complex and pristine PAEU-hGH hydrogel for 1 and 3 days respectively, with a minimal initial burst release compared with hGH alone; these effects are mainly attributed to the formation of ionic complexes between the anionic hGH and cationic PAEU hydrogels and the smaller interconnected pores in the hydrogel.<sup>75</sup>

## 5. LDHs scaffolds in soft tissue engineering

LDHs are biocompatible inorganic biomaterials that have enhanced thermal stability and mechanical strength of the scaffolds. Monika *et al.* fabricated LDH-PVC nanocomposite scaffolds seeded by C3H10t1/2 cells. The hemolysis test showed a positive effect and more blood compatibility on LDHs-functionalized PVC scaffolds than the PVC scaffolds.<sup>75</sup> Lee *et al.* developed a new LDHs/polypeptide thermogel-based nanocomposite system (Fig. 7). RGD-coated LDHs and cartogen (KGN) in poly(ethylene glycol)-poly(L-alanine)-poly(L-aspartate) (PEG-PA-PD) triblock copolymer, network were used. This combination with tonsil-derived mesenchymal stem cells (TMSCs) was proposed as an injectable scaffold for chondrogenic differentiation. TMSCs in PAG-PA-PD scaffold with Mg-Al LDHs retained a significant increase in mRNA and protein levels of type II collagen and SOX9.<sup>76</sup>

Giriprasath *et al.* developed a novel double-layer scaffold made of HAP pellets coated by poly(3-hydroxybutyric acid)-poly(*N*-vinylpyrrolidone) matrix and LDHs (HAP: NFM-LDHs). The nanofibrous bone graft's *in vitro* biocompatibility, and



Fig. 7 2D/3D nanocomposite platform incorporating stem cells, kartogenin (KGN), and RGD-coated LDHs in a poly(ethylene glycol)-poly(L-alanine)-poly(L-aspartate) (PEG-PA-PD) triblock copolymer thermogel for effective chondrogenic differentiation of the stem cells. This figure is reproduced from ref. 76 with permission from American Chemical Society, copyright 2017.



fluorescent activity were examined for 1, 3, 7, and 14 days. MG63 cells showed outstanding cell adhesion and proliferation on both the top and bottom layers of the scaffolds. The nanofibrous matrix resulted in significantly higher cell adhesion from day 3 to 14. Compared to the control of LDHs in the structure, cell adhesion increased significantly on HAP: NFM-LDHs surface. This approach provides the opportunity to perform alternative nanofibrous bone grafts containing Mg–Al LDHs for bone tissue engineering applications.<sup>77</sup> Hsiao *et al.* indicated the possibility that an injectable and thermoresponsive hydrogel would be suitable for gene therapy by using osteoarthritic chondrocytes. They formulated poly(*N*-isopropylacrylamide) (pNIPAAm) hydrogels with Mg–Al or Mg–Fe LDHs by encapsulating siRNA and providing 80–95% siRNA transfection in PNIPAAm/LDHs hybrid hydrogels. Expressions of ACAN, MMP13, Col2A1 genes have been observed. Hydrogels in blend with LDHs may be good candidates specifying both cell delivery and siRNA transfection.<sup>78</sup>

Seyedeh *et al.* have created a new fiber-based biomaterial that can mimic ECM in tissue organ development and regeneration. They combined samples with Mg–Al LDHs ranging from 0.1 wt% to 10 wt% in *in vitro* experiments with stem cells derived from mouse adipose (mADSCs). They also assessed the effects of mADSCs on adhesion, proliferation, and viability, and adipogenic differentiation throughout PCL enrichment with Mg–Al LDHs. The composite electrospun PCL scaffolds had a better cell adhesion and proliferation compared to non-treated PCL. Additionally, a substantial increase in the adipogenic differentiation of mADSCs was obtained. The PCL-LDHs scaffolds with high porosity (94%) indicated numerous possibilities in applying soft tissue engineering.<sup>79</sup>

Due to the complication of the corneal stroma ultrastructure, efficient ECM production is exceptionally challenging. Mojgan *et al.* have created a new poly(urethane-urea) (PUU) based scaffold that can be used in corneal tissue engineering. Zn–Al LDHs were synthesized using the co-precipitation method, laden with vitamin C (VC), and dispersed in the PUU to control VC release. The scaffolds were prepared with electrospinning to mimic the corneal stroma. VC-loaded Zn–Al LDHs allowed the adhesion of the corneal regeneration. According to the *in vitro* effects of three types of experimental groups (PUU, PUU/Zn–Al LDHs, and PUU/VC/Zn–Al LDHs), stromal keratocyte cells exhibited some level of proliferation on the scaffolds through the peak value obtained with PUU/VC/Zn–Al LDHs scaffolds after one week. The results showed significant differences in gene expression. A specific increase was observed in the expression of ALDH3A1 protein, the keratocyte marker, and the expression of ACTA2 gene  $\alpha$ -SMA protein of the myofibroblast phenotype, the sustained release of VC from PUU/VC/Zn–Al LDHs scaffolds. All results suggest that PUU/VC/Zn–Al LDHs scaffolds may be ideal for corneal stromal tissue engineering.<sup>80</sup>

## 6. Future trends and perspectives

LDHs are successful candidates for carrying therapeutic agents due to their high anion exchange capacities and charge densities for next-generation tissue engineering applications. The

advantages such as biocompatibility, biodegradability, tunability, and high loading efficiency of LDH-based drug carriers make this field of study a high priority range and its expansion to other biomedical applications. LDHs contribute to drug release mechanisms *via* a pH-sensitive response, well-regulated particle size, and interlayer spaces. They promise to overcome low bioavailability, improve the thermal and photostability, and sustain and control the release of the active drug, thereby improving their pharmacokinetics and pharmacodynamics. By increasing the effectiveness of the drug, they could reduce the dose of administration as well as reducing the side effects of current pharmaceutical drugs.

Stimuli-responsive nanomaterials have been developed for delivering the drug to tumors. In the tumor hypoxic environment LDHs react with H<sub>2</sub>O<sub>2</sub>, this leads to a change in their structure and then the release of the drug improving the therapeutic efficacy. In the future, LDHs enhanced with nanoparticles could potentially be used in a lower pH medium for faster and accurate tumor target drug delivery. Despite the increase of LDHs applications in cancer research, it is still required to understand LDHs and cells' interaction mechanisms fully. Further studies are required for understanding the activation of the intracellular pathways of the cancer cells and tumor cell apoptosis with the help of the LDHs. Moreover, proteins and antigens could be delivered by LDH nano-vaccines for cancer immunotherapy and to enhance the immune system overall. Another major highlight of the LDHs is their efficacy in delivering genes to the target site. They have been shown capable of transporting DNA and RNA avoiding non-specific sites, some authors suggest that LDHs could be used for transfection methods. Also, organic molecules such as hormones and vitamins can be loaded into the LDHs for controlled release.

Many challenges still exist for LDHs to evolve as a drug delivery system of choice. While the thermosensitive LDHs can be used for anti-HIV drug delivery in the vagina tract, the positively charged LDHs can be a strategy for ocular drug delivery, and its pH-dependent degradation can be a better approach for tumor-targeted drug delivery; the sensitivity of LDHs in an acidic environment is a hurdle in oral drug delivery due to the enzymatic and acidic degradation in the stomach and less absorption from the small intestine, this could be prevented by using polymer coating or other encapsulation methods. Moreover, when administered *via* the blood system they may interact with negatively charge biomolecules in the environment that may lead to loss of surface charge, aggregation, and precipitation, thus, improvement of the LDHs stability is a major challenge. Despite the advances in the modification or functionalization of the surface of the LDHs for major stability, there are a few reports in drug delivery applications. Further studies are required to understand the *in vivo* biodegradability and clearance of LDHs nanomaterials and to include development of ultra-thin LDH nanosheets to avoid pre-mature therapeutic agents release and controlled drug release.

LDHs have been used as composites for regenerative medicine and tissue engineering applications. Herewith, LDHs can create a bio-safe environment around cells and tissue surfaces.



## Review

It is expected that tissue scaffolds should be mimicked like ECM for cell adhesion, intercellular interaction, and cell differentiation during tissue repairing. The absence of infection is essential to accelerate the tissue regeneration in these tissue implants. Thus, the scaffolds' mechanical properties can be tuned by using LDHs to obtain a favorable environment as successful implants with the antibacterial properties of LDHs. Moreover, in bone therapy and regeneration, the release of  $Mg^{+2}$  ions from Mg–Al LDHs, provides an alkaline environment formation and activation of osteogenic differentiation pathways. Furthermore, Mg–Al LDHs can also induce ALP activation of osteoblasts. In the future, to develop the best commercialization for LDHs-based biomaterials in clinic, it is necessary to improve the surface modification, the drug loading, and the synthesis methods to produce highly stable and uniform LHDs with minimal variation in size, geometry, and thickness.

## Conflicts of interest

There are no conflicts to declare.

## Acknowledgements

The Scientific and Technological Research Council of Turkey (TUBITAK) (Grant number 118S549) supported this work.

## References

- 1 M. Goldberg, R. Langer and X. Jia, Nanostructured materials for applications in drug delivery and tissue engineering, *J. Biomater. Sci., Polym. Ed.*, 2007, **18**, 241–268, DOI: 10.1163/156856207779996931.
- 2 X. Liu, M. N. George, S. Park, A. L. Miller II, B. Gaihre, L. Li and L. Lu, 3D-printed scaffolds with carbon nanotubes for bone tissue engineering: Fast and homogeneous one-step functionalization, *Acta Biomater.*, 2020, **111**, 129–140, DOI: 10.1016/j.actbio.2020.04.047.
- 3 R. Yang, S. Yang, K. Li, Z. Luo, B. Xian, J. Tang and J. Ge, Carbon Nanotube Polymer Scaffolds as a Conductive Alternative for the Construction of Retinal Sheet Tissue, *ACS Chem. Neurosci.*, 2021, **12**, 3167–3175, DOI: 10.1021/acscemneuro.1c00242.
- 4 A. F. Girao, J. Sousa, A. Dominguez-Bajo, A. Gonzalez-Mayorga, I. Bdikin, E. Pujades-Otero and P. A. Marques, 3D Reduced Graphene Oxide Scaffolds with a Combinatorial Fibrous-Porous Architecture for Neural Tissue Engineering, *ACS Appl. Mater. Interfaces*, 2020, **12**, 38962–38975, DOI: 10.1021/acsmi.0c10599.
- 5 Z. Li, S. Xiang, Z. Lin, E. N. Li, H. Yagi, G. Cao and H. Lin, Graphene oxide-functionalized nanocomposites promote osteogenesis of human mesenchymal stem cells via enhancement of BMP-SMAD1/5 signaling pathway, *Biomaterials*, 2021, **121**, 121082, DOI: 10.1016/j.biomaterials.2021.121082.
- 6 S. S. Suner, S. Demirci, B. Yetiskin, R. Fakhrullin, E. Naumenko, O. Okay and N. Sahiner, Cryogel composites based on hyaluronic acid and halloysite nanotubes as scaffold for tissue engineering, *Int. J. Biol. Macromol.*, 2019, **130**, 627–635, DOI: 10.1016/j.ijbiomac.2019.03.025.
- 7 E. Naumenko and R. Fakhrullin, Halloysite nanoclay/biopolymers composite materials in tissue engineering, *Biotechnol. J.*, 2019, **14**, 1900055, DOI: 10.1002/biot.201900055.
- 8 E. A. Naumenko, I. D. Guryanov, R. Yendluri, Y. M. Lvov and R. F. Fakhrullin, Clay nanotube–biopolymer composite scaffolds for tissue engineering, *Nanoscale*, 2016, **8**, 7257–7271, DOI: 10.1039/C6NR00641H.
- 9 Z. P. Xu, G. S. Stevenson, C. Q. Lu, G. Q. Lu, P. F. Bartlett and P. P. Gray, Stable suspension of layered double hydroxide nanoparticles in aqueous solution, *J. Am. Chem. Soc.*, 2006, **128**, 36–37, DOI: 10.1021/ja056652a.
- 10 J. Nath, A. Ahmed, P. Saikia, A. Chowdhury and S. K. Dolui, Acrylic acid grafted gelatin/LDH based biocompatible hydrogel with the pH-controllable release of vitamin B12, *Appl. Clay Sci.*, 2020, **190**, 105569, DOI: 10.1016/j.clay.2020.105569.
- 11 J. H. Lee, W. Zhang, H. J. Ryu, G. Choi, J. Y. Choi and J. H. Choy, Enhanced thermal stability and mechanical property of EVA nanocomposites upon addition of organo-intercalated LDH nanoparticles, *Polymer*, 2019, **117**, 274–281, DOI: 10.1016/j.polymer.2019.06.011.
- 12 M. Shamsayei, Y. Yamini, H. Asiabi and M. Safari, On-line packed magnetic in-tube solid-phase microextraction of acidic drugs naproxen and indomethacin by using  $Fe_3O_4@SiO_2@layered$  double hydroxide nanoparticles with high anion exchange capacity, *Microchim. Acta*, 2018, **185**, 192, DOI: 10.1007/s00604-018-2716-7.
- 13 L. Yan, W. Chen, X. Zhu, L. Huang, G. Zhu, Z. Wang, V. A. L. Roy, X. Chen and X. Chen, Folic acid conjugated self-assembled layered double hydroxide nanoparticles for high-efficacy-targeted drug delivery, *Chem. Commun.*, 2013, **49**, 10938–10940, DOI: 10.1039/c3cc45714a.
- 14 S. Dasgupta, Controlled release of ibuprofen using Mg–Al LDH nano carrier, *IOP Conf. Ser.: Mater. Sci. Eng.*, 2017, **225**, 012005, DOI: 10.1088/1757-899X/225/1/012005.
- 15 C. da Costa Fernandes, T. S. Pinto, H. R. Kang, P. de Magalhães Padilha, I. H. J. Koh, V. R. L. Constantino and W. F. Zambuzzi, Layered Double Hydroxides Are Promising Nanomaterials for Tissue Bioengineering Application, *Adv. Biosyst.*, 2019, **3**, 1800238, DOI: 10.1002/adbi.201800238.
- 16 C. Taviot-Guého, V. Prévot, C. Forano, G. Renaudin, C. Mousty and F. Leroux, Tailoring Hybrid Layered Double Hydroxides for the Development of Innovative Applications, *Adv. Funct. Mater.*, 2018, **28**, 1–33, DOI: 10.1002/adfm.201703868.
- 17 F. Fayyazbakhsh, M. Solati-Hashjin, A. Keshtkar, M. A. Shokrgozar, M. M. Dehghan and B. Larijani, Novel layered double hydroxides-hydroxyapatite/gelatin bone tissue engineering scaffolds: Fabrication, characterization, and in vivo study, *Mater. Sci. Eng., C*, 2017, **76**, 701–714, DOI: 10.1016/j.msec.2017.02.172.
- 18 X. S. Li, M. R. Ke, W. Huang, C. H. Ye and J. D. Huang, A pH-responsive layered double hydroxide (LDH)-Phthalocyanine



- nanohybrid for efficient photodynamic therapy, *Chem. - Eur. J.*, 2015, **21**, 3310–3317, DOI: 10.1002/chem.201404514.
- 19 G. Mishra, B. Dash and S. Pandey, Layered double hydroxides: A brief review from fundamentals to application as evolving biomaterials, *Appl. Clay Sci.*, 2018, **153**, 172–186, DOI: 10.1016/j.clay.2017.12.021.
- 20 L. Yan, S. Gonca, G. Zhu, W. Zhang and X. Chen, Layered double hydroxide nanostructures and nanocomposites for biomedical applications, *J. Mater. Chem. B*, 2019, **7**, 5583–5601, DOI: 10.1039/c9tb01312a.
- 21 M. V. Bukhtiyarova, A review on effect of synthesis conditions on the formation of layered double hydroxides, *J. Solid State Chem.*, 2019, **269**, 494–506, DOI: 10.1016/j.jssc.2018.10.018.
- 22 L. P. F. Benício, R. A. Silva, J. A. Lopes, D. Eulálio, R. M. M. dos Santos, L. A. De Aquino, L. Vergütz, R. F. Novais, L. M. Da Costa, F. G. Pinto and J. Tronto, Layered double hydroxides: Nanomaterials for applications in agriculture | Hidróxidos duplos lamelares: Nanomateriais para aplicações na agricultura, *Rev. Bras. Cienc. Solo*, 2015, **39**, 1–13, DOI: 10.1590/0100683rbc20150817.
- 23 Z. Gu, J. J. Atherton and Z. P. Xu, Hierarchical layered double hydroxide nanocomposites: Structure, synthesis and applications, *Chem. Commun.*, 2015, **51**, 3024–3036, DOI: 10.1039/c4cc07715f.
- 24 C. Taviot-Guého, V. Prévot, C. Forano, G. Renaudin, C. Mousty and F. Leroux, Tailoring Hybrid Layered Double Hydroxides for the Development of Innovative Applications, *Adv. Funct. Mater.*, 2018, **28**, 703868, DOI: 10.1002/adfm.201703868.
- 25 T. Baradaran, S. S. Shafiei, S. Mohammadi and F. Moztafzadeh, Poly( $\epsilon$ -caprolactone)/layered double hydroxide microspheres-aggregated nanocomposite scaffold for osteogenic differentiation of mesenchymal stem cell, *Mater. Today Commun.*, 2020, **23**, 100913, DOI: 10.1016/j.mtcomm.2020.100913.
- 26 C. da Costa Fernandes, T. S. Pinto, H. R. Kang, P. de Magalhães Padilha, I. H. J. Koh, V. R. L. Constantino and W. F. Zambuzzi, Layered Double Hydroxides Are Promising Nanomaterials for Tissue Bioengineering Application, *Adv. Biosyst.*, 2019, **3**, 1–14, DOI: 10.1002/adbi.201800238.
- 27 M. Mehra, M. A. Asadollahi, K. Ghaedi, H. Salehi and A. Arpanaei, Electrospun aligned PLGA and PLGA/gelatin nanofibers embedded with silica nanoparticles for tissue engineering, *Int. J. Biol. Macromol.*, 2015, **79**, 687–695, DOI: 10.1016/j.ijbiomac.2015.05.050.
- 28 M. Baek, I. S. Kim, J. Yu, H. E. Chung, J. H. Choy and S. J. Choi, Effect of different forms of anionic nanoclays on cytotoxicity, *J. Nanosci. Nanotechnol.*, 2011, **11**, 1803–1806, DOI: 10.1166/jnn.2011.3408.
- 29 S. J. Choi, J. M. Oh and J. H. Choy, Toxicological effects of inorganic nanoparticles on human lung cancer A549 cells, *J. Inorg. Biochem.*, 2009, **103**, 463–471, DOI: 10.1016/j.jinorgbio.2008.12.017.
- 30 N. Sultana and T. H. Khan, In vitro degradation of PHBV scaffolds and nHA/PHBV composite scaffolds containing hydroxyapatite nanoparticles for bone tissue engineering, *J. Nanomater.*, 2012, **2012**, 190950, DOI: 10.1155/2012/190950.
- 31 L. Qin, S. Wang, R. Zhang, R. Zhu, X. Sun and S. Yao, Two different approaches to synthesizing Mg-Al-layered double hydroxides as folic acid carriers, *J. Phys. Chem. Solids*, 2008, **69**, 2779–2784, DOI: 10.1016/j.jpcs.2008.06.144.
- 32 A. U. Kura, S. H. H. Al Ali, M. Z. Hussein, S. Fakurazi and P. Arulselvan, Development of a controlled-release anti-parkinsonian nanodelivery system using levodopa as the active agent, *Int. J. Nanomed.*, 2013, **8**, 1103–1110, DOI: 10.2147/IJN.S39740.
- 33 L. Qin, M. Xue, W. Wang, R. Zhu, S. Wang, J. Sun, R. Zhang and X. Sun, The in vitro and in vivo antitumor effect of layered double hydroxides nanoparticles as delivery for podophyllotoxin, *Int. J. Pharm.*, 2010, **388**, 223–230, DOI: 10.1016/j.ijpharm.2009.12.044.
- 34 F. Barahuie, M. Z. Hussein, S. H. Hussein-Al-Ali, P. Arulselvan, S. Fakurazi and Z. Zainal, Preparation and controlled-release studies of a protocatechuic acid-magnesium/aluminumlayered double hydroxide nanocomposite, *Int. J. Nanomed.*, 2013, **8**, 1975–1987, DOI: 10.2147/IJN.S42718.
- 35 L. Qin, M. Wang, R. Zhu, S. You, P. Zhou and S. Wang, The in vitro sustained release profile and antitumor effect of etoposide-layered double hydroxide nanohybrids, *Int. J. Nanomed.*, 2013, **8**, 2053–2064, DOI: 10.2147/IJN.S43203.
- 36 M. Ramli, M. Z. Hussein and K. Yusoff, Preparation and characterization of an anti-inflammatory agent based on a zinc-layered hydroxide-salicylate nanohybrid and its effect on viability of Vero-3 cells, *Int. J. Nanomed.*, 2013, **8**, 297–306, DOI: 10.2147/IJN.S38858.
- 37 A. U. Kura, P. S. Cheah, M. Z. Hussein, Z. Hassan, T. I. Tengku Azmi, N. F. Hussein and S. Fakurazi, Toxicity evaluation of zinc aluminium levodopa nanocomposite via oral route in repeated dose study, *Nanoscale Res. Lett.*, 2014, **9**, 1–11, DOI: 10.1186/1556-276X-9-261.
- 38 A. U. Kura, S. H. Hussein-Al-Ali, M. Z. Hussein and S. Fakurazi, Preparation of Tween 80-Zn/Al-levodopa-layered double hydroxides nanocomposite for drug delivery system, *Sci. World J.*, 2014, **2014**, 104246, DOI: 10.1155/2014/104246.
- 39 Y. Wu, R. Zhu, Y. Zhou, J. Zhang, W. Wang, X. Sun, X. Wu, L. Cheng, J. Zhang and S. Wang, Layered double hydroxide nanoparticles promote self-renewal of mouse embryonic stem cells through the PI3K signaling pathway, *Nanoscale*, 2015, **7**, 11102–11114, DOI: 10.1039/c5nr02339d.
- 40 Y. Wu, R. Zhu, X. Ge, X. Sun, Z. Wang, W. Wang, M. Wang, H. Liu and S. Wang, Size-dependent effects of layered double hydroxide nanoparticles on cellular functions of mouse embryonic stem cells, *Nanomedicine*, 2015, **10**, 3469–3482, DOI: 10.2217/nnm.15.158.
- 41 S. Y. Kwak, Y. J. Jeong, J. S. Park and J. H. Choy, Bio-LDH nanohybrid for gene therapy, *Solid State Ionics*, 2002, **151**, 229–234, DOI: 10.1016/S0167-2738(02)00714-2.
- 42 F. Peng, D. Wang, D. Zhang, H. Cao and X. Liu, The prospect of layered double hydroxide as bone implants: A study of



- mechanical properties, cytocompatibility and antibacterial activity, *Appl. Clay Sci.*, 2018, **165**, 179–187, DOI: 10.1016/j.clay.2018.08.020.
- 43 S. J. Choi, J. M. Oh and J. H. Choy, Safety aspect of inorganic layered nanoparticles: Size-dependency in vitro and in vivo, *J. Nanosci. Nanotechnol.*, 2008, **8**, 5297–5301, DOI: 10.1166/jnn.2008.1143.
- 44 V. R. R. Cunha, R. B. De Souza, A. M. C. R. P. Da Fonseca Martins, I. H. J. Koh and V. R. L. Constantino, Accessing the biocompatibility of layered double hydroxide by intramuscular implantation: Histological and microcirculation evaluation, *Sci. Rep.*, 2016, **6**, 1–10, DOI: 10.1038/srep30547.
- 45 S. Wang, Z. Zhang, L. Dong, G. I. N. Waterhouse, Q. Zhang and L. Li, A remarkable thermosensitive hydrogel cross-linked by two inorganic nanoparticles with opposite charges, *J. Colloid Interface Sci.*, 2019, **538**, 530–540, DOI: 10.1016/j.jcis.2018.12.012.
- 46 G. R. Jiménez-Gastélum, E. M. Aguilar-Medina, E. Soto-Sainz, R. Ramos-Payán and E. L. Silva-Benítez, Antimicrobial Properties of Extracellular Matrix Scaffolds for Tissue Engineering, *BioMed Res. Int.*, 2019, **2019**, 9641456, DOI: 10.1155/2019/9641456.
- 47 R. Florencio-Silva, G. R. D. S. Sasso, E. Sasso-Cerri, M. J. Simões and P. S. Cerri, Biology of Bone Tissue: Structure, Function, and Factors That Influence Bone Cells, *BioMed Res. Int.*, 2015, **2015**, 421746, DOI: 10.1155/2015/421746.
- 48 S. Wu, X. Liu, K. W. K. Yeung, C. Liu and X. Yang, Biomimetic porous scaffolds for bone tissue engineering, *Mater. Sci. Eng., R*, 2014, **80**, 1–36, DOI: 10.1016/j.mser.2014.04.001.
- 49 Y. Xie, Y. He, P. L. Irwin, T. Jin and X. Shi, Antibacterial activity and mechanism of action of zinc oxide nanoparticles against *Campylobacter jejuni*, *Appl. Environ. Microbiol.*, 2011, **77**, 2325–2331, DOI: 10.1128/AEM.02149-10.
- 50 M. Li, L. Li and S. Lin, Efficient antimicrobial properties of layered double hydroxide assembled with transition metals via a facile preparation method, *Chin. Chem. Lett.*, 2019, **31**, 1511–1515, DOI: 10.1016/j.ccl.2019.09.047.
- 51 B. Saifullah, M. E. El Zowalaty, P. Arulselvan, S. Fakurazi, T. J. Webster, B. M. Geilich and M. Z. Hussein, Antimycobacterial, antimicrobial, and biocompatibility properties of para-aminosalicylic acid with zinc layered hydroxide and Zn/Al layered double hydroxide nanocomposites, *Drug Des., Dev. Ther.*, 2014, **8**, 1029–1036, DOI: 10.2147/DDDT.S63753.
- 52 B. F. C. A. Gohi, H. Y. Zeng, S. Xu, K. M. Zou, B. Liu, X. L. Huang and X. J. Cao, Optimization of znal/chitosan supra-nano hybrid preparation as efficient antibacterial material, *Int. J. Mol. Sci.*, 2019, **20**, 5705–5705, DOI: 10.3390/ijms20225705.
- 53 W. De Zhang, Y. M. Zheng, Y. Sen Xu, Y. X. Yu, Q. S. Shi, L. Liu, H. Peng and Y. Ouyang, Preparation and antibacterial property of waterborne polyurethane/Zn-Al layered double hydroxides/ZnO nanocomposites, *J. Nanosci. Nanotechnol.*, 2013, **13**, 409–416, DOI: 10.1166/jnn.2013.6912.
- 54 Y. Zhao, C. J. Wang, W. Gao, B. Li, Q. Wang, L. Zheng, M. Wei, D. G. Evans, X. Duan and D. O'Hare, Synthesis and antimicrobial activity of ZnTi-layered double hydroxide nanosheets, *J. Mater. Chem. B*, 2013, **1**, 5988–5994, DOI: 10.1039/c3tb21059f.
- 55 M. Yadollahi, H. Namazi and M. Aghazadeh, Antibacterial carboxymethyl cellulose/Ag nanocomposite hydrogels cross-linked with layered double hydroxides, *Int. J. Biol. Macromol.*, 2015, **79**, 269–277, DOI: 10.1016/j.ijbiomac.2015.05.002.
- 56 G. Carja, Y. Kameshima, A. Nakajima, C. Dranca and K. Okada, Nanosized silver-anionic clay matrix as nanostructured ensembles with antimicrobial activity, *Int. J. Antimicrob. Agents*, 2009, **34**, 534–539, DOI: 10.1016/j.ijantimicag.2009.08.008.
- 57 A. M. Youssef, H. Moustafa, A. Barhoum, A. E. F. A. Hakim and A. Dufresne, Evaluation of the Morphological, Electrical and Antibacterial Properties of Polyaniline Nanocomposite Based on Zn/Al-Layered Double Hydroxides, *ChemistrySelect*, 2017, **2**, 8553–8566, DOI: 10.1002/slct.201701513.
- 58 M. Li, Y. Sultanbawa, Z. P. Xu, W. Gu, W. Chen, J. Liu and G. Qian, High and long-term antibacterial activity against *Escherichia coli* via synergy between the antibiotic penicillin G and its carrier ZnAl layered double hydroxide, *Colloids Surf., B*, 2019, **174**, 435–442, DOI: 10.1016/j.colsurfb.2018.11.035.
- 59 P. Morissette Martin, K. Creber and D. W. Hamilton, *Measuring gene expression changes on biomaterial surfaces*, Elsevier Ltd, 2017, pp. 111–131, DOI: DOI: 10.1016/B978-0-08-100603-0.00006-7.
- 60 K. A. Long, J. K. Jackson, C. Yang, B. Chehroudi, D. M. Brunette and H. M. Burt, Controlled release of alendronate from polymeric films, *J. Biomater. Sci., Polym. Ed.*, 2009, **20**, 653–672, DOI: 10.1163/156856209X426457.
- 61 H. R. Kang, C. J. da Costa Fernandes, R. A. da Silva, V. R. L. Constantino, I. H. J. Koh and W. F. Zambuzzi, Mg-Al and Zn-Al Layered Double Hydroxides Promote Dynamic Expression of Marker Genes in Osteogenic Differentiation by Modulating Mitogen-Activated Protein Kinases, *Adv. Healthcare Mater.*, 2018, **7**, 1–12, DOI: 10.1002/adhm.201700693.
- 62 J. Zhang, X. Ma, D. Lin, H. Shi, Y. Yuan, W. Tang, H. Zhou, H. Guo, J. Qian and C. Liu, Magnesium modification of a calcium phosphate cement alters bone marrow stromal cell behavior via an integrin-mediated mechanism, *Biomaterials*, 2015, **53**, 251–264, DOI: 10.1016/j.biomaterials.2015.02.097.
- 63 J. Tan, D. Wang, H. Cao, Y. Qiao, H. Zhu and X. Liu, Effect of Local Alkaline Microenvironment on the Behaviors of Bacteria and Osteogenic Cells, *ACS Appl. Mater. Interfaces*, 2018, **10**, 42018–42029, DOI: 10.1021/acsami.8b15724.
- 64 H. Kang, M. Kim, Q. Feng, S. Lin, K. Wei, R. Li, C. J. Choi, T. H. Kim, G. Li, J. M. Oh and L. Bian, Nanolayered hybrid mediates synergistic co-delivery of ligand and ligation



- activator for inducing stem cell differentiation and tissue healing, *Biomaterials*, 2017, **149**, 12–28, DOI: 10.1016/j.biomaterials.2017.09.035.
- 65 F. Fayyazbakhsh, M. Solati-Hashjin, A. Keshtkar, M. A. Shokrgozar, M. M. Dehghan and B. Larijani, Novel layered double hydroxides-hydroxyapatite/gelatin bone tissue engineering scaffolds: Fabrication, characterization, and in vivo study, *Mater. Sci. Eng., C*, 2017, **76**, 701–714, DOI: 10.1016/j.msec.2017.02.172.
- 66 D. Cao, Z. Xu, Y. Chen, Q. Ke, C. Zhang and Y. Guo, Ag-loaded MgSrFe-layered double hydroxide/chitosan composite scaffold with enhanced osteogenic and antibacterial property for bone engineering tissue, *J. Biomed. Mater. Res., Part B*, 2018, **106**, 863–873, DOI: 10.1002/jbm.b.33900.
- 67 H. Huang, J. Xu, K. Wei, Y. J. Xu, C. K. K. Choi, M. Zhu and L. Bian, Bioactive Nanocomposite Poly(Ethylene Glycol) Hydrogels Cross-linked by Multifunctional Layered Double Hydroxides Nanocrosslinkers, *Macromol. Biosci.*, 2016, 1019–1026, DOI: 10.1002/mabi.201600054.
- 68 L. Tamaro, V. Vittoria, A. Calarco, O. Petillo, F. Riccitiello and G. Peluso, Effect of layered double hydroxide intercalated with fluoride ions on the physical, biological and release properties of a dental composite resin, *J. Dent.*, 2014, **42**, 60–67, DOI: 10.1016/j.jdent.2013.10.019.
- 69 M. Chakraborti, J. K. Jackson, D. Plackett, D. M. Brunette and H. M. Burt, Drug intercalation in layered double hydroxide clay: Application in the development of a nanocomposite film for guided tissue regeneration, *Int. J. Pharm.*, 2011, **416**, 305–313, DOI: 10.1016/j.ijpharm.2011.06.016.
- 70 Q. Li, D. Wang, J. Qiu, F. Peng and X. Liu, Regulating the local pH level of titanium: Via Mg-Fe layered double hydroxides films for enhanced osteogenesis, *Biomater. Sci.*, 2018, **6**, 1227–1237, DOI: 10.1039/c8bm00100f.
- 71 Y. X. Chen, R. Zhu, Q. F. Ke, Y. S. Gao, C. Q. Zhang and Y. P. Guo, MgAl layered double hydroxide/chitosan porous scaffolds loaded with PFT $\alpha$  to promote bone regeneration, *Nanoscale*, 2017, **9**, 6765–6776, DOI: 10.1039/c7nr00601b.
- 72 X. Wang, H. Y. Kua, Y. Hu, K. Guo, Q. Zeng, Q. Wu, H. H. Ng, G. Karsenty, B. De Crombrughe, J. Yeh and B. Li, P53 Functions As a Negative Regulator of Osteoblastogenesis, Osteoblast-Dependent Osteoclastogenesis, and Bone Remodeling, *J. Cell Biol.*, 2006, **172**, 115–125, DOI: 10.1083/jcb.200507106.
- 73 F. Fayyazbakhsh, M. Solati-Hashjin, A. Keshtkar, M. A. Shokrgozar, M. M. Dehghan and B. Larijani, Release behavior and signaling effect of vitamin D3 in layered double hydroxides-hydroxyapatite/gelatin bone tissue engineering scaffold: An in vitro evaluation, *Colloids Surf., B*, 2017, **158**, 697–708, DOI: 10.1016/j.colsurfb.2017.07.004.
- 74 N. K. Singh, Q. V. Nguyen, B. S. Kim and D. S. Lee, Nanostructure controlled sustained delivery of human growth hormone using injectable, biodegradable, pH/temperature responsive nanobiohybrid hydrogel, *Nanoscale*, 2015, **7**, 3043–3054, DOI: 10.1039/c4nr05897f.
- 75 M. Singh, R. K. Singh, S. K. Singh, S. K. Mahto and N. Misra, In vitro biocompatibility analysis of functionalized poly(vinyl chloride)/layered double hydroxide nanocomposites, *RSC Adv.*, 2018, **8**, 40611–40620, DOI: 10.1039/C8RA06175K.
- 76 S. S. Lee, G. E. Choi, H. J. Lee, Y. Kim, J. H. Choy and B. Jeong, Layered Double Hydroxide and Polypeptide Thermogel Nanocomposite System for Chondrogenic Differentiation of Stem Cells, *ACS Appl. Mater. Interfaces*, 2017, **9**, 42668–42675, DOI: 10.1021/acsami.7b17173.
- 77 G. Ramanathan, L. S. Liji, P. Fardim and U. T. Sivagnanam, Fabrication of 3D dual-layered nanofibrous graft loaded with layered double hydroxides and their effects in osteoblastic behavior for bone tissue engineering, *Process Biochem.*, 2018, **64**, 255–259, DOI: 10.1016/j.procbio.2017.09.025.
- 78 H. Y. Yang, R. J. Van Ee, K. Timmer, E. G. M. Craenmehr, J. H. Huang, F. C. Öner, W. J. A. Dhert, A. H. M. Kragten, N. Willems, G. C. M. Grinwis, M. A. Tryfonidou, N. E. Papen-Botterhuis and L. B. Creemers, A novel injectable thermoresponsive and cytocompatible gel of poly(N-isopropylacrylamide) with layered double hydroxides facilitates siRNA delivery into chondrocytes in 3D culture, *Acta Biomater.*, 2015, **23**, 214–228, DOI: 10.1016/j.actbio.2015.05.018.
- 79 S. S. Shafiei, M. Shavandi, G. Ahangari and F. Shokrolahi, Electrospun layered double hydroxide/poly( $\epsilon$ -caprolactone) nanocomposite scaffolds for adipogenic differentiation of adipose-derived mesenchymal stem cells, *Appl. Clay Sci.*, 2016, **127–128**, 52–63, DOI: 10.1016/j.clay.2016.04.004.
- 80 M. Moghanizadeh-Ashkezari, P. Shokrollahi, M. Zandi, F. Shokrolahi, M. J. Daliri, M. R. Kanavi and S. Balaghali, Vitamin C Loaded Poly(urethane-urea)/ZnAl-LDH Aligned Scaffolds Increase Proliferation of Corneal Keratocytes and Up-Regulate Vimentin Secretion, *ACS Appl. Mater. Interfaces*, 2019, **11**, 35525–35539, DOI: 10.1021/acsami.9b07556.

